Molecular Biology of the Cell
Vol. 19, 1185–1198, March 2008

Role of Insulin Receptor and Balance in Insulin Receptor Isoforms A and B in Regulation of Apoptosis in Simian Virus 40-immortalized Neonatal Hepatocytes

Carmen Nevado,* Manuel Benito,* and Angela M. Valverde†

*Departamento de Bioquimica y Biologia Molecular II, Facultad de Farmacia, Universidad Complutense, 28040 Madrid, Spain; and †Instituto de Investigaciones Biomédicas "Alberto Sols," Consejo Superior de Investigaciones Científicas and Universidad Autónoma de Madrid, 28029 Madrid, Spain

Submitted May 18, 2007; Revised December 11, 2007; Accepted December 26, 2007
Monitoring Editor: M. Bishr Omary

We have investigated the unique role of the insulin receptor (IR) and the balance of its isoforms A and B in the regulation of apoptosis in simian virus 40 (SV40)-immortalized neonatal hepatocytes. Immortalized hepatocytes lacking (HIR KO) or expressing the entire IR (HIR LoxP), and cells expressing either IRA (HIR RecA) or IRB (HIR RecB) have been generated. IR deficiency in hepatocytes increases sensitivity to the withdrawal of growth factors, because these cells display an increase in reactive oxygen species, a decrease in Bcl-x_L, a rapid accumulation of nuclear Foxo1, and up-regulation of Bim. These events resulted in acceleration of caspase-3 activation, DNA laddering, and cell death. The single expression of either IRA or IRB produced a stronger apoptotic phenotype. In these cells, protein complexes containing IRA or IRB and Fas/Fas-associating protein with death domain activated caspase-8, and, ultimately, caspase-3. In hepatocytes expressing IRA, Bid cleavage and cytochrome C release were increased whereas direct activation of caspase-3 by caspase-8 and a more rapid apoptotic process occurred in hepatocytes expressing IRB. Conversely, coexpression of IRA and IRB in IR-deficient hepatocytes rescued from apoptosis. Our results suggest that balance alteration of IRA and IRB may serve as a ligand-independent apoptotic trigger in hepatocytes, which may regulate liver development.

INTRODUCTION

In the liver, regulation of apoptosis is essential for development and hepatic homeostatic mechanisms (Schulte-Hermann *et al*., 1997). Thus, liver hyperplasia during development or regeneration may be compensated by inhibition of apoptosis. Conversely, enhanced liver cell death and impaired regeneration are typical features of most liver disorders (Patel *et al*., 1998). Activation of death receptors such as Fas and tumor necrosis factor (TNF)-α, mitochondrial damage, and oxidative stress of the endoplasmic reticulum are the major triggers of apoptosis that ultimately produce liver damage (Ockner, 2001). In fact, in many instances hepatic failure may represent the deregulation of hepatic homeostasis because of an imbalance between damaging and protective signals that are tightly regulated under physiological conditions.

Progression of the apoptotic program can be inhibited at different levels depending on the origin of the death stimulus. Insulin promotes survival in a number of cell types, including hepatocytes (Valverde *et al*., 2004), by a complex network of intracellular signaling pathways. The cascade begins when the activated insulin receptor (IR) β-chain phosphorylates IRS proteins and then activates the phosphatidylinositol 3-kinase/Akt signaling pathway, which plays a central role in both the survival and metabolic actions elicited by insulin (Kennedy *et al*., 1997).

Alternative splicing of the 36 nucleotide exon 11 of the IR α-subunit results in the expression of two isoforms: IRA (lacking exon 11) and IRB (including exon 11) (Seino and Bell, 1989). The relative abundance of the mRNAs encoding IRA and IRB isoforms displays tissue specificity in both humans and rats (Moller *et al*., 1989, Goldstein and Dudley, 1990). Additionally, IR isoform expression is also regulated by stage of development and by cell differentiation, with IRA representing the predominant isoform in fetal tissues and cancer cells (Frasca *et al*., 1999). In contrast, IRB is expressed mainly in the insulin-responsive tissues such as liver that maintain glucose homeostasis. Accordingly, a switch from IRA to IRB induced by dexamethasone in a hepatoma cell line correlated with increased insulin sensitivity (Kosaki and Webster, 1993). However, no information is available regarding the roles of IRA and IRB in the regulation of cellular apoptosis in the liver. In this regard, the development of experimental systems allowing differential expression or suppression of either isoform is critical in understanding the role of IR isoforms. Therefore, in the present study, we have investigated whether IR and its isoforms A and B are implicated in the signals that induce programmed cell death in hepatocytes. As a model system, we have used simian virus 40 (SV40)-immortalized neonatal hepatocyte cell lines recently generated in our laboratory (Nevado *et al*., 2006). These include control (HIR LoxP) and IR-deficient (HIR KO) cells, and hepatocytes expressing IR

This article was published online ahead of print in *MBC in Press* (http://www.molbiolcell.org/cgi/doi/10.1091/mbc.E07–05–0473) on January 2, 2008.

Address correspondence to: Angela M. Valverde (avalverde@iib.uam.es) or Manuel Benito (benito@farm.ucm.es).

Abbreviations used: FS, fetal serum; IGF-IR, insulin-like growth factor I receptor; IR, insulin receptor; PAGE, polyacrylamide gel electrophoresis; PBS, phosphate-buffered saline; PCR, polymerase chain reaction.

isoforms A (HIR RecA) and B (HIR RecB) of IR. Our data clearly demonstrate that the lack of IR sensitizes neonatal hepatocytes to death signals induced by serum withdrawal. This effect is reverted by coexpression of IRA and IRB isoforms in IR-deficient cells. Unexpectedly, the imbalance of IR isoforms in immortalized neonatal hepatocytes, generated by the individual expression of IRA or IRB in IR-deficient cells, produced a more severe apoptotic phenotype. This enhanced apoptosis was due to the formation of protein complexes between IR isoforms and the Fas/Fas-associating protein with death domain (FADD) death machinery, thereby triggering a strong activation of caspase-8–mediated cell death.

MATERIALS AND METHODS

Reagents

Fetal calf serum (FS) and culture media were obtained from Invitrogen (Carlsbad, CA). Insulin, hygromycin, and the anti-β-actin antibody were from Sigma-Aldrich (St. Louis, MO). Anti-Bcl-x_L (556499), anti-Bim (559685), anti-cytochrome *c* (556433), the agonist anti-Fas (15401D), and the anti-Fas conjugated with fluorescein isothiocyanate (554258) antibodies were from BD Biosciences PharMingen (San Diego, CA). Anti-Bid antibody (AF860) was from R&D Systems (Minneapolis, MN). Anti-IR (sc-711) and anti-caspase-8 (sc-7980) antibodies and Syrian hamster immunoglobulin G (IgG) (sc-2713) were from Santa Cruz Biotechnology (Santa Cruz, CA). Anti-phospho-Akt (Ser473; 9271), anti-phospho-extracellular signal-regulated kinase (ERK) (Thr 202/Tyr 204; 9101), anti-Akt (9272), anti-ERK (9102), and anti-Foxo1 (9462) antibodies were purchased from Cell Signaling Technology (Beverly, MA). Anti-FADD (M033-3; Clone 1F7) was from MBL International (Watertown, MA). All other reagents used were of the purest grade available.

Generation of SV40-immortalized HIR LoxP and HIR KO Hepatocyte Cell Lines

Primary hepatocytes were obtained from livers of 3-d-old IRLoxP mice (homozygous for a floxed allele of exon 4 of the IR) (Michael *et al*., 2000) and further submitted to collagenase dispersion and primary culture as described previously (Fabregat *et al*., 1989). Viral Bosc-23 packaging cells were transfected at 70% confluence by calcium phosphate coprecipitation with 3 μg/6-cm dish of the puromycin-resistance retroviral vector pBabe encoding K1mutant of SV40 Large T antigen (kindly provided by J. de Caprio, Dana-Farber Cancer Institute, Boston, MA). Primary hepatocytes were infected at 60% confluence with 4 μg/ml polybrene-supplemented virus for 48 h and maintained in culture medium for 72 h, before selection with 1 μg/ml puromycin for 3 wk. Then, immortalized cell lines were generated and further cultured for 10–15 d with arginine-free medium supplemented with 10% FBS to avoid growth of nonparenchymal cells. For in vitro recombination of the IR, immortalized hepatocytes (IRLoxP) were first cultured to 70–80% confluence. After 24 h, cells were infected with adenoviruses encoding *cre* recombinase at a titer of 10^9 plaque-forming units. After 1 h, growing medium was added for a further 48 h. Individual colonies were selected and deletion of IR was assessed by Western blot. In addition, these cells (HIR KO) were cloned twice and resubmitted to viral infection to ensure complete IR deletion.

The immortalized cell lines generated by this protocol have hepatocyte phenotype, because these cells expressed albumin (a plasma protein secreted exclusively by hepatocytes) together with carbamoyl phosphate synthase (an urea cycle marker), and cytokeratine 18 (a cytoskeletal marker of epithelial cells) (Supplemental Figure 1). As a negative control, we performed immunofluorescence experiments with SV40-immortalized β cells previously generated in our laboratory (Guillén *et al*., 2006). Immunofluorescence was not detected in these immortalized β cells. Moreover, the absence of vimentin (a cytoskeletal marker characteristic of fibroblasts) staining demonstrated the absence of fibroblasts in immortalized hepatocyte cell lines.

Rescue of HIR KO Immortalized Hepatocytes by Retroviral Infection with IRA, IRB, or Both Isoforms of IR

Coding sequences for the individual spliced isoforms of the human IR either containing or lacking exon 11 (isoforms B and A, respectively), cloned into pBABE-hygro retroviral vector, were a gift of C. R. Kahn (Joslin Diabetes Center, Boston, MA). Viral particles were obtained as described previously (Valverde *et al*., 2003). HIR KO hepatocytes were infected with 4 μg/ml polybrene-supplemented virus for 48 h and then placed in selection medium containing 200 μg/ml hygromycin for at least 2 wk. Pools of infected cells with similar levels of IR expression were selected to avoid clonal variability. As a control, HIR KO hepatocytes were infected with viral particles expressing empty vector (pBabe hygro). To analyze endogenous (mouse) and reconstituted (human) IR isoforms in immortalized hepatocytes by polymerase chain reaction (PCR), 5 μg of total RNA was primed with deoxythymidine in the presence of murine mammary tumor virus reverse transcriptase (Invitrogen) to synthesize cDNA. The samples were diluted fivefold, and 5% of the total volume was used for subsequent PCR. Primers used were mouse IR exon 11 primer 1, 5′-ATCAGAGTGAGTATGACGACTCGG-3′ and primer 2, 5′-TCCTGACTTGTGGGCACAATGGTA-3′ and human IR exon 11 primer 1, 5′ ACCAGAGTGAGTATGAGGATTCGG-3′ and primer 2, 5′-TCCGGACTCGT-GGGCACGCTGGTC-3′. PCR reactions were performed as described previously (Entingh *et al*., 2003). Reaction products were resolved on 2% agarose gels.

Immunofluorescence and Confocal Imaging

Cells were grown in glass coverslips until 80% confluence was reached. Then, cells were washed twice with phosphate-buffered saline (PBS), fixed in methanol (−20°C) for 2 min, and processed to immunofluorescence. Anti-IR or anti-Foxo1 antibodies were applied for 1 h at 37°C in PBS, 1% bovine serum albumin (BSA), followed by four washes of 5 min each in PBS, a 45-min incubation with fluorescence-conjugated antibody (cyanine [Cy]3-conjugated and fluorescein isothiocyanate [FITC]-conjugated goat anti-rabbit, respectively), and four final washes of 5 min each in PBS. Immunofluorescence was examined in an MRC-1024 confocal microscope (Bio-Rad, Hempstead, United Kingdom) adapted to an inverted Nikon Eclipse TE 300 microscope. Immunofluorescence mounting medium was from Vector Laboratories (Burlingame, CA). Images were taken with 488-nm laser excitation for FITC-conjugated antibodies and 514-nm laser excitation for Cy3-conjugated antibodies. Fluorescence emissions were detected through a 513/24-nm bandpass filter for FITC and a 605/15-nm bandpass filter for Cy3.

Extraction of Nuclear Proteins

Cells were resuspended at 4°C in 10 mM HEPES-KOH, pH 7.9, 1.5 mM $MgCl_2$, 10 mM KCl, 0.5 mM dithiothreitol (DTT), 0.2 mM phenylmethylsulfonyl fluoride (PMSF), 0.75 μg/ml leupeptin, and 0.75 μg/ml aprotinin (buffer A), allowed to swell on ice for 10 min, and then vortexed for 10 s. Samples were centrifuged, and the supernatant containing the cytosolic fraction was stored at −70°C. The pellet was resuspended in cold buffer C (20 mM HEPES-KOH, pH 7.9, 25% glycerol, 420 mM NaCl, 1.5 mM $MgCl_2$, 0.2 mM EDTA, 0.5 mM DTT, 0.2 mM PMSF, 0.75 μg/ml leupeptin, and 0.75 μg/ml aprotinin) and incubated on ice for 20 min for high salt extraction. Cellular debris was removed by centrifugation for 2 min at 4°C, and the supernatant fraction was stored at −70°C.

Isolation of Mitochondrial and Cytosolic Extracts

At the end of the culture time, cells were scrapped off, collected by centrifugation at 2500 × *g* for 5 min at 4°C, and resuspended in hypotonic isolation buffer (1 mM EDTA, 10 mM HEPES, and 50 mM sucrose, pH 7.6). Then, cells were incubated at 37°C for 5 min and homogenized under a Teflon pestle (Overhead Stirrer; Wheaton Instruments, Millville, NJ). Hypertonic isolation buffer (1 mM EDTA, 10 mM HEPES, and 450 mM sucrose, pH 7.6) was added to balance the buffer's tonicity. Samples were centrifuged at 10,000 × *g* for 10 min and the pellets, containing the mitochondrial fraction, were resuspended in lysis buffer. The supernatants contained the cytosolic protein fraction. Cytochrome *c* was analyzed by Western blotting after electrophoresis separation of 50 μg of cytosolic proteins in 15% polyacrylamide-SDS gels.

Protein Determination

Protein determination was performed by the Bradford dye method, using the Bio-Rad reagent and BSA as the standard.

Immunoprecipitation and Western Blotting

To obtain total cell lysates, cells from supernatants were collected by centrifugation at 2000 × *g* for 5 min at 4°C. Attached cells were scraped off in ice-cold PBS, pelleted by centrifugation at 4000 × *g* for 10 min at 4°C, and resuspended in lysis buffer (25 mM HEPES, 2.5 nM EDTA, 0.1% Triton X-100, 1 mM phenylmethylsulfonyl fluoride, and 5 μg/ml leupeptin). Samples were sonicated 30 s at 1.5 mA, and lysates were clarified by centrifugation at 12,000 × *g* for 10 min. For immunoprecipitation, equals amount of protein (600 μg–1 mg) were immunoprecipitated at 4°C with the corresponding antibodies and isotype control serum. The immune complexes were collected on protein A-agarose or protein G-agarose beads and submitted to SDS-PAGE. Then, gels were transferred to Immobilon membranes, and they were blocked using 5% nonfat dried milk or 3% BSA in 10 mM Tris-HCl, and 150 mM NaCl, pH 7.5, and incubated overnight with several antibodies as indicated in 0.05% Tween 20, 10 mM Tris-HCl, and 150 mM NaCl, pH 7.5. Immunoreactive bands were visualized using the ECL Western blotting protocol (GE Healthcare, Little Chalfont, Buckinghamshire, United Kingdom).

Analysis of DNA Laddering

To assess the fragmentation of extranuclear DNA, a modified version of the method of Lyons *et al*. (1992) was used. Cells were washed twice with ice-cold PBS, and then they were scraped and pelleted at 4°C. Cells were resuspended in 500 μl of buffer containing 10 mM EDTA, 0.25% Triton X-100, and 2.5 mM Tris-HCl, pH 8, and stored at 4°C for 15 min. Intact nuclei were pelleted and eliminated by centrifugation at 500 × *g* at 4°C for 30 min, and the supernatant was centrifuged at 25,000 × *g* at 4°C for 15 min. DNA in the supernatant was precipitated at −80°C after the addition of 2 volumes of ethanol (70% final concentration), pelleted by microcentrifugation at 4°C for 15 min, dried, resuspended in 200 μl of 10 mM Tris-HCl, 1 mM EDTA, pH 8 (TE buffer), and incubated at 37°C for 30 min with 0.1 mg/ml RNase A and for 2–3 h with 0.24 mg/ml proteinase K. DNA was purified by phenol-chloroform extraction and precipitated at −70°C after adding (1/10 volume) 3 M sodium acetate, pH 5.3, and (2 volume) ethanol. Precipitated DNA was dissolved in TE buffer containing 30% glycerol, 1 μg/ml ethidium bromide and electrophoresed in a 1.5% agarose gel. Gel was visualized and photographed under transmitted UV light with a Polaroid camera.

Quantification of Apoptotic Cells by Flow Cytometry

After induction of apoptosis, adherent and nonadherent cells were collected by centrifugation, washed with PBS, and fixed with cold ethanol (70%, vol/vol). The cells were then washed, resuspended in PBS, and incubated with RNAse (25 μg/10^6 cells) for 30 min at 37°C. After addition of 0.05% propidium iodide, cells were analyzed by flow cytometry.

Determination of Reactive Oxygen Species (ROS)

Cellular reactive oxygen species were quantified by the dichlorofluorescin (DCFH) assay by using a microplate reader (Wang and Joseph, 1999). This parameter gives a very good evaluation of the degree of cellular oxidative stress, and it has been described previously (Alia *et al*., 2006). Briefly, 2.5×10^5 cells were seeded in six-well plates in growing medium (DMEM plus 10% FS) and cultured to 80% confluence. Then, cells were loaded with 5 μM DCFH for 30 min. After two washes with PBS, cells were cultured in growing medium (control) or serum-free medium for several time periods. Then, fluorescence was quantified in a microplate fluorimeter (Synergy HT; Bio-Tek Instruments, Winooski, VT), and a fair estimation of the overall oxygen species generated per well under the different conditions was obtained. Alternatively, cellular fluorescence was examined under the same experimental conditions in the confocal microscope. Images were taken with 488-nm laser excitation and 510-nm for emission.

Analysis of Caspase-3 Activity

Cells were scraped off, collected by centrifugation at 2500 × *g* for 5 min, and lysed at 4°C in 5 mM Tris-HCl, pH 8.0, 20 mM EDTA, and 0.5% Triton X-100. Lysates were clarified by centrifugation at 13,000 × *g* for 10 min. Reaction mixture contained 25 μl of cellular lysates, 325 μl of assay buffer (20 mM HEPES, pH 7.5, 10% glycerol, and 2 mM dithiothreitol) and 20 μM caspase-3 substrate (Ac-DEVD-AMC). After 2-h incubation in the dark, enzymatic activity was measured in a luminescence spectrophotometer (LS-50; PerkinElmer Life and Analytical Sciences, Boston, MA) (λ excitation, 380 nm; λ emission, 440 nm). We define a unit of caspase-3 activity as the amount of active enzyme necessary to produce an increase in 1 arbitrary unit in the fluorimeter after 2-h incubation with the reaction mixture. Then, protein concentration of cell lysates was determined, and final expression of the results is presented as caspase-3 activity per microgram of total protein.

Analysis of Caspase-8 Activity

Caspase 8-activity was measured with the ApoAlert caspase-8 fluorescent assay kit (K2028; Clontech, Mountain View, CA) accordingly with the manufacturer's instructions by using 7-amino-4-trifluoromethyl coumarin (IETD-AFC) as a substrate. Then, protein concentration of cell lysates was determined, and final expression of the results is presented as caspase-8 activity per microgram of total protein. For the determination of IR-associated caspase-8 activity, cells were lysed in lysis buffer described above for caspase-3 activity. Equal amounts of protein (600 μg) were immunoprecipitated with the anti-IR antibody. The resulting immune complexes were collected on protein A-agarose beads. After three washes with PBS, beads were resuspended in 50 μl of caspase-8 reaction cocktail [20 mM piperazine-*N*,*N*′-bis(2-ethanesulfonic acid), 100 mM NaCl, 10 mM DTT, 1 mM EDTA, 0.1% 3-[(3-cholamidopropyl)dimethylammonio]propanesulfonate, and 10% sucrose] supplemented with 1 μg of Ac-IETD-AFC as a substrate. After 2-h incubation at 37°C, caspase-8 activity was measured in a luminescence spectrophotometer (LS-50) (λ excitation, 380 nm; λ emission, 440 nm).

Cytometric Quantification of Fas Expression

Cells were grown in DMEM plus 10% FS, and then they were trypsinized, washed, resuspended in PBS (1–1.5 × 10^6 cells/assay), and incubated for 30 min at 4°C with 2.5 μg of the anti-Fas antibody Jo2 conjugated with fluorescein isothiocyanate. After washing, cells were incubated with 0.005% propidium iodide and analyzed in the cytometer. The relative fluorescence intensity was recorded as a measure of the amount of Fas expression per cell.

Statistical Analysis

Statistically significant differences between mean values were determined using paired Student's *t* test. Differences were considered statistically significant at $p < 0.05$.

RESULTS

Effect of IR Deficiency or Expression of Isoforms A or B of the IR on Apoptosis in SV40-immortalized Neonatal Hepatocytes upon Serum Withdrawal

Immortalized hepatocyte cell lines with (HIR LoxP) or without IR (HIR KO) and cells encoding for IR isoforms A (HIR RecA) or B (HIR RecB) were obtained and characterized as described in *Materials and Methods*. Figure 1A shows the deletion of IR in HIR KO cells and the re-expression of IRA and IRB by immunofluorescence and reverse transcription-polymerase chain reaction (RT-PCR). The expression of IR at the protein level, as assessed by Western blot, was comparable between HIR LoxP and HIR RecB cell lines, with only a slight increase (0.5-fold) of IRA expressed in HIR RecA immortalized hepatocytes. Of note, due to the small difference in size between both IR isoforms (1.2 kDa), it was not possible to detect endogenous IRA and IRB by Western blot. Moreover, the expression of insulin-like growth factor (IGF)-IR did not change between the four cell lines. Noteworthy, the levels of IR isoforms in HIR LoxP SV40-immortalized neonatal hepatocytes were similar to those observed in SV40-immortalized hepatocytes from wild-type (WT) mice.

Our first goal was to analyze the effect of IR deficiency on the susceptibility of these immortalized hepatocytes to undergo apoptosis upon growth factors withdrawal. Accordingly, HIR LoxP and HIR KO cells were deprived of serum for various periods. Subsequently, DNA cleavage (180-base pair ladder) was analyzed by electrophoresis of extranuclear DNA. HIR LoxP hepatocytes revealed DNA fragmentation after 16 h of serum deprivation (Figure 1B). In contrast, hepatocytes lacking the IR (HIR KO) displayed DNA fragmentation after 8 h of serum withdrawal, indicating that these cells are more sensitive to serum deprivation; thus, apoptosis was induced earlier than in control cells. To determine whether IR splice isoforms A and B modulate the susceptibility to apoptosis in immortalized neonatal hepatocytes, HIR RecA and HIR RecB cells were serum deprived for the same times and DNA laddering was analyzed. Unexpectedly, the unique expression of either IRA or IRB increased sensitivity rather than rescued from apoptosis in response to serum deprivation compared with those cells lacking IR, as revealed by DNA laddering (Figure 1B).

Next, we measured the percentage of apoptosis by analyzing cells with DNA content lower than 2C by flow cytometry during the time course of serum deprivation. In HIR LoxP hepatocytes, 16 h of serum deprivation increased the percentage of hypodiploid cells compared with cells cultured with 10% FS (Figure 1C). DNA laddering pattern pointed out that the lack of IR increased the percentage of apoptotic cells at an earlier time (8 h). Moreover, the individual expression of IRA or IRB isoform in IR-deficient immortalized hepatocytes augmented the number of apoptotic cells at 8 and 16 h of serum deprivation compared with HIR KO hepatocytes. Of note, this effect was more pronounced in HIR RecB cells. To demonstrate that the effects seen in HIR RecA and HIR

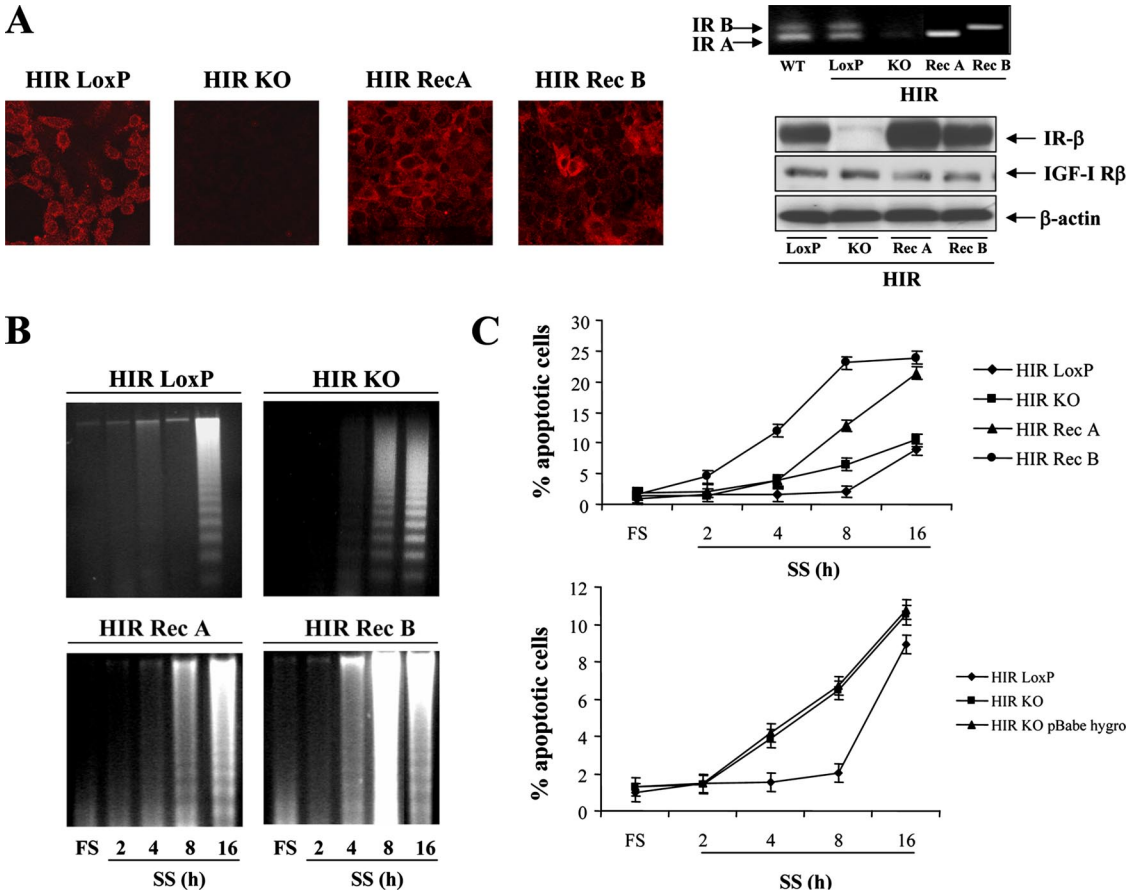

Figure 1. Differential time course of apoptosis in HIR LoxP, HIR KO, HIR KO, pBabe hygro, HIR RecA, and HIR RecB immortalized hepatocytes. (A) Left, HIR KO hepatocytes were infected with retroviruses encoding IRA and IRB isoforms, and hygromycin-resistant pools were expanded. Immunofluorescence detection of IR in growing (10% FS) HIR LoxP, HIR KO, and HIR KO neonatal hepatocytes reconstituted with isoforms A (HIR RecA) and B (HIR RecB) of the IR. Right, total RNA was isolated from HIR LoxP, HIR KO, HIR RecA, HIR RecB, and WT immortalized neonatal hepatocytes, and RT-PCR was performed as described in *Materials and Methods*. A representative experiment is shown. The IR isoforms A and B are indicated by an arrow. Total cell lysates were prepared and analyzed by Western blot with the antibodies against IR and IGF-IR. Representative immunoblots are shown. (B) Immortalized hepatocytes (HIR LoxP, HIR KO, HIR RecA, and HIR RecB), cultured in 10% FS, were serum-deprived for 2–16 h. Then, cells were scraped and subjected to extranuclear DNA extraction. Purified DNA was electrophoresed and visualized by UV fluorescence after staining with ethidium bromide. A representative of three experiments is shown. (C) Cells (HIR LoxP, HIR KO, HIR KO pBabe hygro, HIR RecA, and HIR RecB), were serum deprived as described in B. The percentage of cells with DNA lower than 2C (apoptotic cells) was determined by flow cytometry as described in *Materials and Methods*. Results are the mean ± SE (n = 5).

RecB cells were not caused by the infection procedure, we generated a control cell line by retroviral infection of HIR KO immortalized hepatocytes with empty vector (HIR KO pBabe hygro). Then, the percentage of apoptotic cells was analyzed at the same times of growth factors withdrawal. As shown in Figure 1C (bottom), no differences in the percentage of apoptotic cells were found between HIR KO hepatocytes and those cells infected with pBabe hygro.

Insulin Signaling through Akt and ERK Rescued HIR LoxP, HIR RecA, and HIR RecB, but not HIR KO, Immortalized Hepatocytes from Apoptosis

We have previously shown that insulin is a survival factor that rescues wild-type SV40-immortalized neonatal hepatocytes from serum withdrawal-induced apoptosis. At the molecular level, both Akt and ERK signaling pathways have been implicated in the survival effect of insulin or IGF-I in a number of cell types, including immortalized hepatocytes (Valverde *et al*., 2004). To analyze the phosphorylation of Akt and ERK in HIR loxP, HIR KO, HIR RecA, and HIR RecB immortalized hepatocytes, cells were cultured to 90% confluence and then they were serum starved for 4 h. Subsequently, cells were stimulated with 10 nM insulin for a further 10 min. The phosphorylation of Akt and ERK was observed in HIR loxP, HIR RecA and HIR RecB immortalized hepatocytes upon insulin stimulation (Figure 2A). As expected, the lack of IR totally abolished insulin-stimulated activation of Akt and ERK in both HIR KO and HIR KO pBabe hygro cells. Interestingly, the phosphorylation of Akt and ERK in response to IGF-I stimulation was similar in all cell lines (data not shown). Next, we examined whether insulin was able to suppress serum withdrawal-induced apoptosis in our lines of immortalized hepatocytes. For these studies, cells were incubated for 16 h in serum-free medium in the absence or presence of 10 nM insulin. Insulin significantly decreased the percentage of apoptotic cells and DNA laddering in HIR LoxP, HIR RecA, and HIR RecB hepatocytes cultured in serum-free medium (Figure 2B). How-

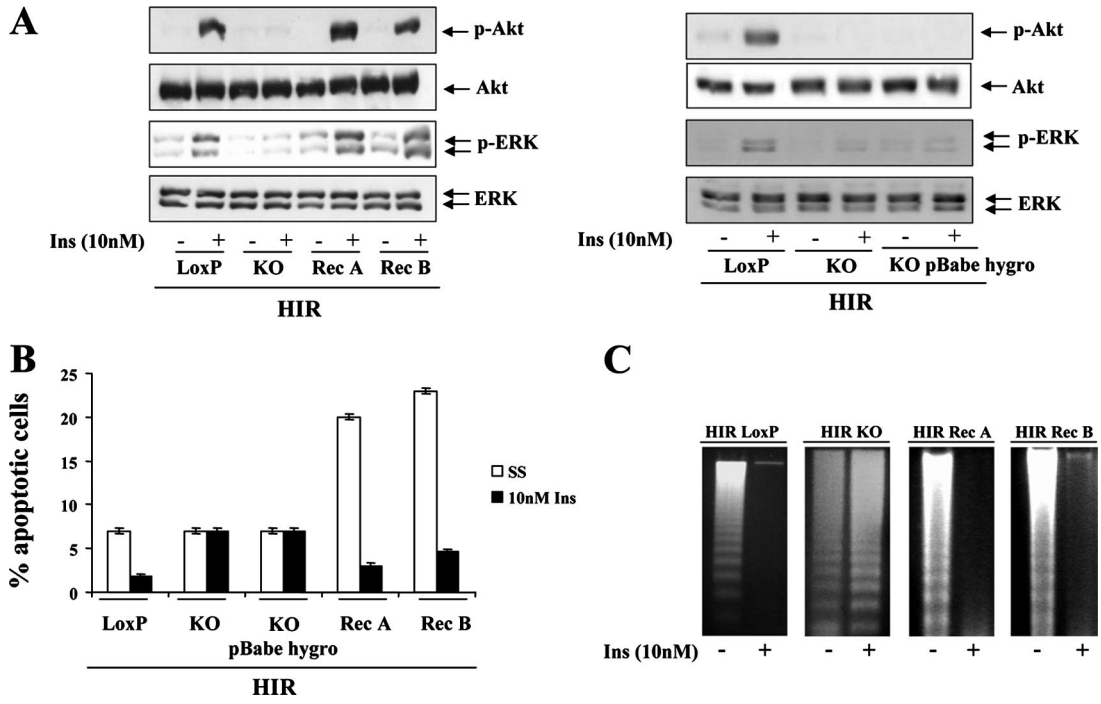

Figure 2. Insulin protected HIR LoxP, HIR RecA, and HIR RecB, but not HIR KO, immortalized hepatocytes from apoptosis through activation of Akt and ERK signaling pathways. (A) Left, immortalized hepatocytes were cultured in DMEM plus 10% FS to 90% confluence, and then they were serum starved for 4 h. Cells were stimulated with 10 nM insulin for 10 min. Control cells were cultured in the absence of the hormone. At the end of the culture time, cells were lysed, and total protein (50 μg) was analyzed by Western blot with the anti-phospho-Akt (Ser473) and phospho ERK (Thr 202/Tyr 204) antibodies. The autoradiograms shown are representative of three experiments. Right, the same experiment was performed in HIR KO pBabe hygro immortalized hepatocytes. (B) Cells were cultured in serum-free medium without or with 10 nM insulin for 16 h. Some dishes were cultured in growing medium (10% FS). At the end of the culture time, the percentage of cells with DNA lower than 2C (apoptotic cells) was determined by flow cytometry as described in *Materials and Methods*. Results are expressed as percentage of apoptotic cells and are means ± SE from three independent experiments with duplicate dishes. (C) Cells were cultured as described above. At the end of the culture time, cells were scraped and subjected to extranuclear DNA extraction. Purified DNA was electrophoresed and visualized by UV fluorescence after staining with ethidium bromide. A representative of three experiments is shown.

ever, insulin failed to exert a survival effect on cells lacking IR, as expected.

IR Deficiency Increased ROS in SV40-immortalized Neonatal Hepatocytes: Protection by Expression of IRA or IRB Isoforms

Next, we investigated the molecular mechanisms responsible for the increased susceptibility to apoptosis in immortalized IR-deficient hepatocytes and cells expressing IRA or IRB. Direct evaluation of the ROS is a very good indication of the oxidative damage to living cells (Wang and Joseph, 1999). Thus, we investigated whether the increased sensitivity to growth factors withdrawal induced by IR deficiency or individual expression of IRA or IRB isoforms in neonatal hepatocytes could be related to alterations in levels of ROS. When HIR LoxP hepatocytes were incubated in serum-free medium, we noted a time-dependent increase in the intracellular oxidation state (Figure 3A). Interestingly, IR deficiency provoked a dramatic increase in ROS levels in a time-dependent manner. By contrast, ROS levels were significantly lower in response to serum withdrawal in immortalized hepatocytes expressing either IRA or IRB isoform, reaching values similar to control (HIR LoxP) hepatocytes. Figure 3B shows a representative staining of ROS levels in cells deprived of growth factors for 4 h.

Effect of IR Deficiency or IRA or IRB Isoforms on the Expression of the Bcl-2 Proteins in SV40-immortalized Hepatocytes upon Serum Withdrawal

In an attempt to elucidate the molecular basis for the increase in apoptosis provoked by IR deficiency or by the individual expression of IRA or IRB isoforms in immortalized hepatocytes, we studied the levels of pro- and antiapoptotic proteins of the Bcl-2 family, which are implicated in mitochondrial changes during apoptosis. First, we analyzed the endogenous expression of Bim, Bid, and Bcl-x_L in the four lines of immortalized hepatocytes under normal culture conditions (DMEM supplemented with 10% FS). As shown in Figure 4A, the endogenous expression of the proapoptotic proteins Bim and Bid did not differ between cell lines. However, the expression of the anti-apoptotic protein Bcl-x_L was down-regulated in IR-deficient hepatocytes (HIR KO), and it remained at low levels even after reconstitution with IRA or IRB. Next, cells were deprived of serum for several times to examine the expression of the proapoptotic member Bim, which is positively modulated by serum withdrawal in immortalized hepatocytes (Valverde *et al*., 2004). Although Bim expression was low in all cell types under growth conditions, it gradually increased in HIR LoxP hepatocytes upon serum deprivation (Figure 4B). This induction of Bim was accelerated by the lack of IR (HIR KO cells), being detected as early as 2 h

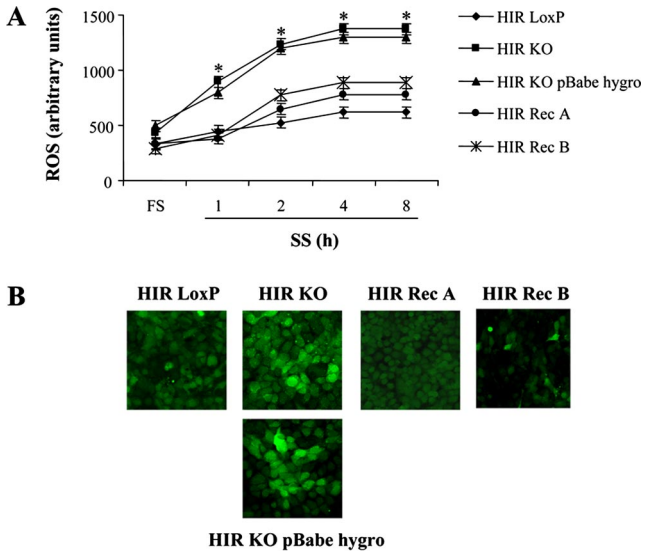

Figure 3. Deletion of IR in immortalized hepatocytes increases ROS: protection by reconstitution with IRA and IRB isoforms. (A) Cells (HIR LoxP, HIR KO, HIR KO pBabe hygro, HIR RecA, and HIR RecB) were serum deprived for 1–8 h. Then, ROS were quantified by the DCFH assay as described in *Materials and Methods*. Results, expressed as arbitrary units, are means ± SE from two independent experiments with triplicate dishes. Statistical analysis was carried out by Student's *t* test by comparison between IR-deficient hepatocytes (HIR KO and HIR KO pBabe hygro) and HIR LoxP, HIR RecA, and HIR RecB cells (*$p < 0.05$). (B) ROS levels were visualized by confocal microscopy in cells deprived of growth factors for 4 h. Representative images of two independent experiments performed in duplicate are shown.

after serum withdrawal. Interestingly, in serum-deprived HIR RecA or HIR RecB hepatocytes, the expression pattern of Bim was similar to that observed in HIR KO cells. Of note, serum withdrawal did not modify Bcl-x_L expression in any of our immortalized hepatocyte cell lines (data not shown).

Nuclear Translocation of Foxo1 and Activation of Caspase-8 in HIR KO, HIR RecA, or HIR RecB Hepatocytes upon Serum Withdrawal

Transcription factors of the Foxo family have recently been implicated in the regulation of several proapoptotic genes, including mitochondria-associated proteins such as Bim and members of the death receptor pathway such as FasL (Dijkers *et al*., 2000; Suhara *et al*., 2002). Growth factor stimulation induces phosphorylation of Foxo1 by PKB/Akt, thereby precluding its entry into the nucleus (Nakae *et al*., 2000). In fact, we have recently demonstrated that serum withdrawal provokes the accumulation of Foxo1 into the nucleus of wild-type immortalized hepatocytes in a time-dependent manner (Valverde *et al*., 2004). Therefore, in the present study, we assessed whether the subcellular distribution of Foxo1 represents one of the mechanisms by which IR deficiency or the expression of IRA or IRB isoforms in hepatocytes increases susceptibility to apoptosis. Under growing conditions, Foxo1 in nuclear extracts was almost undetectable in all the cell lines (Figure 5A). However, substantial differences were noted between the cell lines in response to serum withdrawal. Whereas Foxo1 was detected in nuclear extracts after 8 h of serum deprivation in HIR LoxP hepatocytes, the lack of IR accelerated the time course of Foxo1 nuclear translocation such that we detected it in nuclear extracts after only 2 h of serum-free conditions. Similar results were obtained when we analyzed nuclear Foxo1 in cells expressing IRA or IRB. All nuclear fractions were assumed to be pure as cytosolic p85α was not detected by Western blotting of these preparations (data not shown). To substantiate these data, we performed immunofluorescence analysis in cells cultured under nonapoptotic (DMEM plus 10% FS) and apoptotic (serum-free DMEM) conditions. To visualize Foxo1 subcellular distribution we performed this experi-

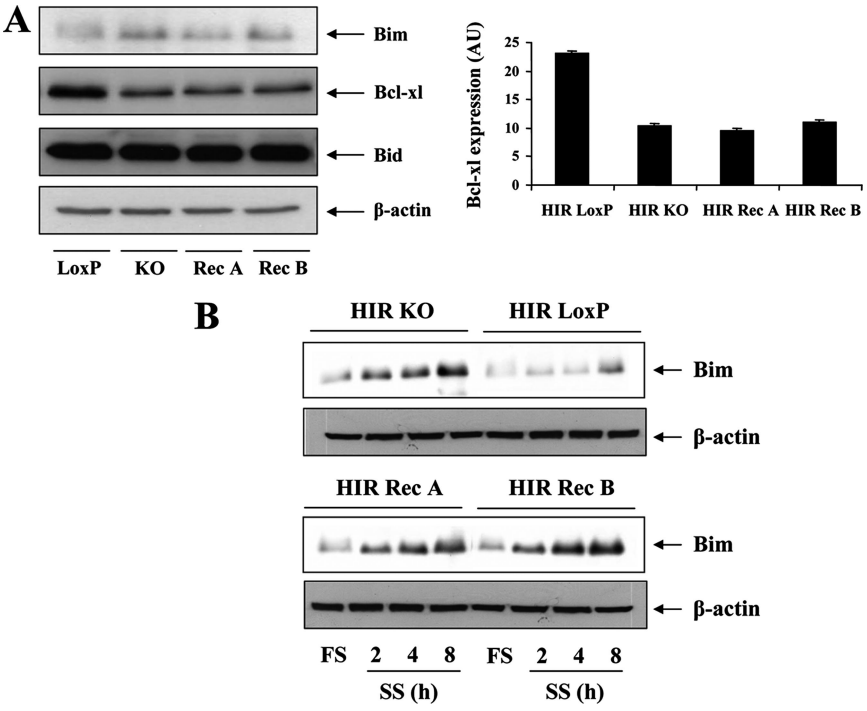

Figure 4. Differential effects of serum deprivation on the expression of Bcl-2 family proteins in HIR LoxP, HIR KO, HIR RecA, and HIR RecB immortalized hepatocytes. (A) Cells were cultured in growing medium until 90% confluence. The endogenous expression of Bim, Bcl-x_L, and Bid was analyzed by Western blot. A representative experiment is shown. The autoradiograms corresponding to Bcl-x_L expression were quantitated by scanning densitometry, and results are means ± SE from three independent experiments. (B) Cells were serum-deprived for the indicated times. Total protein (50 μg) was used for Western blot analysis with the antibodies against Bim and β-actin for protein loading. A representative experiment is shown.

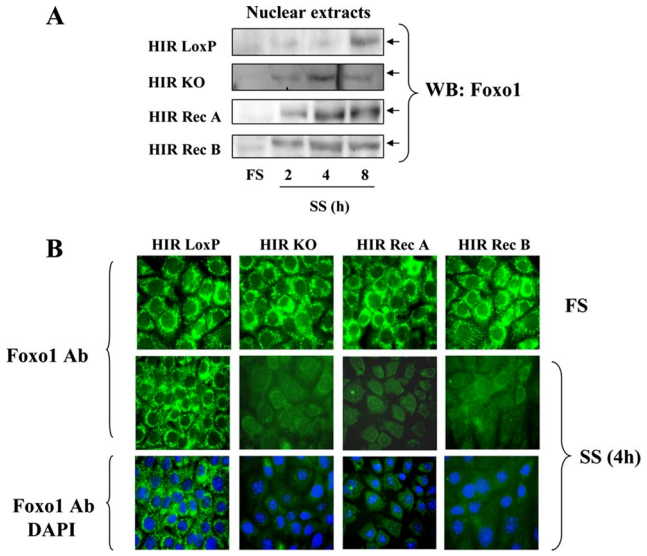

Figure 5. Time course of nuclear translocation of Foxo1 in HIR LoxP, HIR KO, HIR RecA, and HIR RecB immortalized hepatocytes. (A) Cells were cultured in growing medium until 80% confluence. Then, cells were maintained in growing medium (FS) or serum-deprived (SS) at the indicated times. At the end of the culture time, attached and nonattached cells were collected and total cell lysates and nuclear extracts were prepared. Nuclear protein (50 μg) was submitted to Western blot analysis with the anti-Foxo1 antibody. A representative experiment out of three is shown. (B) The subcellular localization of Foxo1 was analyzed by immunofluorescence in immortalized hepatocytes cultured under growing conditions or in serum-free medium for 4 h. Representative images corresponding to three independent experiments are shown.

ment at 4 h of serum deprivation based on the differences found in the biochemical analysis. As shown in Figure 5B, in the absence of the apoptotic trigger Foxo1 staining was visualized in the cytosol with a strong signal in the perinuclear area. However, 4 h of growth factors withdrawal resulted in the loss of the perinuclear staining and the presence of immunofluorescence signal in the nucleus in HIR KO, HIR RecA, HIR RecB cells. A similar pattern of immunofluorescence has been previously shown in SV40-immortalized IRS-2–deficient hepatocytes (Valverde *et al.*, 2004).

Recently, it has been proposed that nuclear Foxo proteins induce the death receptor pathway by activating the FasL gene promoter (Suhara *et al.*, 2002). Subsequently, the clustering of Fas in response to the binding of FasL leads to caspase-8-dependent cell death (Juo *et al.*, 1998). To assess whether IR-dependent differences in the regulation of Foxo1 translocation concur with effects on caspase-8 activation, we measured caspase-8 activity during the time course of serum deprivation. HIR LoxP cells displayed a modest increase in caspase-8 activity upon serum withdrawal (Figure 6A). When IR was deleted (HIR KO and HIR KO pBabe hygro), caspase-8 activity was slightly higher than in HIR LoxP cells, reaching the maximal value (2-fold) at 8 h. These results indicate that the acceleration of nuclear translocation of Foxo1 would contribute to the slight increase in caspase-8 activity in IR-deficient hepatocytes. Unexpectedly, caspase-8 activity was much higher when IRA or IRB were expressed individually in immortalized hepatocytes reaching maximal values of 3.5- and 5-fold, respectively, at 8 h.

Next, we assessed the relevance of caspase-8 activation in the apoptosis observed in HIR RecA or HIR RecB hepatocytes. Cells were serum deprived for 8 h in the absence or presence of the specific caspase-8 inhibitor IETD (20 μM), and caspase-8 activity and the percentage of apoptotic cells were analyzed. As shown in Figure 6B, IETD totally blunted caspase-8 activity in both kind of cells (left) and significantly inhibited the percentage of apoptotic cells (right). These results indicate that elevated caspase-8 activity by a Foxo1-independent mechanism is mediating the increased susceptibility to undergo apoptosis in hepatocytes expressing individually either IRA or IRB.

Immortalized Hepatocytes Expressing IRA or IRB Isoforms Associated Caspase-8 Activity, Fas, and FADD upon Serum Withdrawal, but Only Isoform A Induced Bid Cleavage

The fact that caspase-8 activity was highly elevated in serum-deprived immortalized hepatocytes expressing either IRA or IRB prompted us to explore the possibility that caspase-8 activity might associate with protein complexes containing these IR isoforms. To test this hypothesis, HIR LoxP, HIR KO, HIR KO pBabe hygro, HIR RecA, and HIR RecB hepatocytes were serum deprived for 8 h or maintained in medium with 10% FS. Adherent and nonadherent cells were then collected and lysed. Equals amount of protein (600 μg) were immunoprecipitated with the anti-IR antibody and then we assayed for caspase-8 activity in the immune complexes as described in *Materials and Methods*. Caspase-8 activity was detected in the immunoprecipitates from serum deprived HIR RecA or HIR RecB cells (Figure 7A). By contrast, IR-associated caspase-8 activity was not detected in serum-deprived HIR loxP, HIR KO, and HIR KO pBabe hygro hepatocytes.

Given these results, we next investigated whether IRA or IRB might form complexes with the death receptor Fas/CD95 that is a potential apoptotic trigger in hepatocytes (Malhi *et al.*, 2006). Using the same experimental conditions as described above, cell lysates were immunoprecipitated with the anti-Fas antibody, and the resulting immune complexes were analyzed by Western blot by using the anti-IR antibody. As depicted in Figure 7B (top), coimmunoprecipitation of Fas with the IR was observed under basal conditions in HIR RecA or HIR RecB hepatocytes cultured in 10% FS. When these cells were changed to serum-free medium, we detected an increase in Fas-associated IRA and IRB, suggesting that serum deprivation promotes formation of these complexes. By contrast, Fas was not detected in IR immunoprecipitations from growing HIR LoxP and HIR KO immortalized hepatocytes. Next, we performed the same experiment using the anti-FADD antibody for immunoprecipitation followed by Western blotting for IR. The results shown in Figure 7B (top) reveal the presence of FADD/IRA or FADD/IRB complexes in hepatocytes expressing IRA or IRB but not in HIR LoxP hepatocytes or in the negative control HIR KO. Moreover, the abundance of these complexes increased upon serum withdrawal. The immunoprecipitations performed with isotype control serum demonstrated the specificity of these immune complexes (Figure 7B, middle). In addition, basal expression of FADD and caspase-8 and the percentage of positive cells for Fas staining were similar in all kind of cells (Figure 7B, bottom). As activated caspase-8 results in Bid cleavage, we analyzed the presence of the truncated Bid (tBid) fragment. Figure 7C shows the presence of detectable levels of tBid in HIR RecA hepatocytes deprived of trophic factors for 8 h. By contrast, in HIR RecB cells tBid was barely detected.

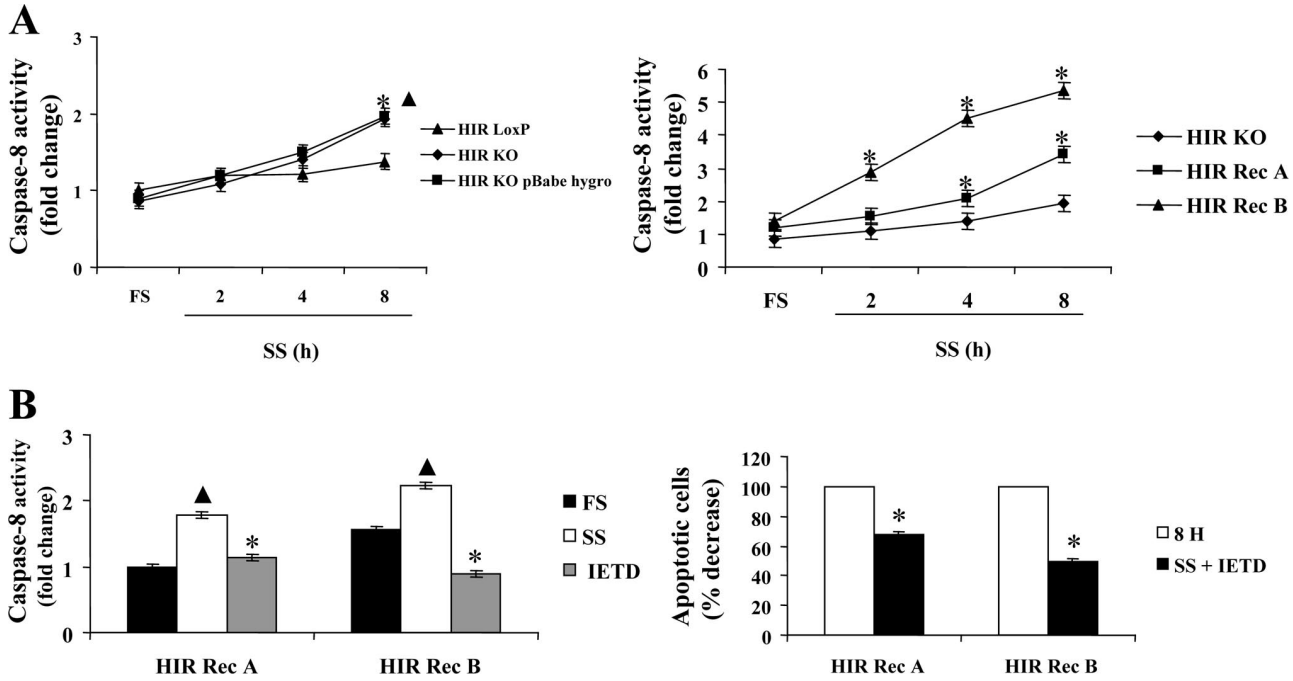

Figure 6. Time course of caspase-8 activation in HIR LoxP, HIR KO, HIR RecA, and HIR RecB immortalized hepatocytes. (A) Cells were serum deprived for 2–8 h. At the end of the culture time, cells were collected and lysed. Caspase-8 activity was measured as described in *Materials and Methods*. The value corresponding to HIR LoxP hepatocytes, cultured in DMEM plus 10% FS, was set to 1. Results are expressed as -fold change of caspase-8 activity, and are means ± SE from three independent experiments with duplicate dishes. Statistical analysis was carried out by Student's *t* test by comparison between IR-deficient hepatocytes (HIR KO and HIR KO pBabe hygro) and HIR LoxP cells (left) and between HIR RecA and HIR RecB hepatocytes and HIR KO cells (right) (▲, *$p < 0.05$). (B) Left, HIR RecA and HIR RecB hepatocytes were cultured for 8 h in serum-free medium without or with 20 μM IETD. At the end of the culture time, caspase-8 activity was measured. The value corresponding to HIR RecA cells, cultured in DMEM plus 10% FS, was set to 1. Results are expressed as -fold change of caspase-8 activity, and they are means ± SE from three independent experiments with duplicate dishes. Statistical analysis was carried out by Student's *t* test by comparison between cells treated without and with IETD (▲, * $p < 0.05$). Right, cells were serum-deprived as described above. The percentage of cells with DNA lower than 2C (apoptotic cells) was determined by flow cytometry. The value corresponding to serum-deprived cells was set to 100%. Results are expressed as percentage of decrease of apoptotic cells in the presence of IETD, and they are means ± SE from three independent experiments with duplicate dishes. Statistical analysis was carried out by Student's *t* test by comparison between cells without and with IETD (*$p < 0.05$).

Effect of IR Deficiency and the Expression of IRA or IRB Isoform on Cytochrome c Mitochondrial Release and Caspase-3 Activation in Immortalized Hepatocytes

The release of cytochrome *c* from the mitochondria is a point of convergence between intrinsic (mitochondrial-mediated) and extrinsic (death receptor-mediated) apoptotic pathways. Therefore, we evaluated whether the release of cytochrome *c* from mitochondria to cytosol in response to growth factors withdrawal was much affected by deletion of IR or the expression of IRA or IRB in immortalized hepatocytes. To analyze this, cells were cultured in serum-free medium for 2–8 h, and subsequently, subcellular fractions of mitochondria and cytosol were prepared. Cytochrome *c* content decreased considerably in the mitochondria, occurring in the cytosol after 4 h of serum withdrawal in HIR LoxP cells (Figure 8A). In the absence of IR, cytosolic cytochrome *c* occurred at an earlier time (2 h), followed by a plateau. In HIR RecB hepatocytes, the time course of cytochrome *c* release was similar to that of HIR KO cells. Conversely, in hepatocytes expressing IRA isoform the amount of cytochrome *c* in the cytosol significantly increased following 8 h of serum deprivation. No cytochrome *c* oxidase was detected in the cytosolic extracts (data not shown).

Finally, we determined caspase-3 activity, a common point of convergence between the extrinsic and intrinsic apoptotic pathways, during the time course of serum deprivation in our cell lines. In HIR LoxP hepatocytes, serum deprivation triggered a gradual increase in the activation of caspase-3 (Figure 8B). However, in the absence of trophic factors, we detected higher enzymatic activity at earlier times (4 h) in hepatocytes lacking IR (HIR KO and HIR KO pBabe hygro). Interestingly, the expression of either IRA or IRB in hepatocytes increased the basal levels of caspase-3 activity and that induced by serum withdrawal; after 8 h of serum deprivation, caspase-3 activity was fourfold (HIR IRA) or fivefold (HIR IRB) higher than when grown in 10% FS. This significant increase in caspase-3 activity in response to 8 h of serum deprivation was totally blocked by treatment with the caspase-8 inhibitor IETD.

Coexpression of IRA and IRB in IR-deficient Immortalized Hepatocytes Reverted the Susceptibility to Undergo Apoptosis upon Growth Factors Deprivation

To allow the conclusion that an imbalance of IR isoforms is an apoptotic trigger in immortalized neonatal hepatocytes, we coexpressed both isoforms in HIR KO cells. For that goal, HIR KO hepatocytes were infected with retroviruses encoding IRA and IRB. After hygromycin selection, we obtained cell lines (HIR RecAB) with comparable IRA and IRB levels than that of HIR LoxP hepatocytes, and comparable IR protein levels (Figure 9A). Then, HIR RecAB cells were stimulated with insulin and, as shown in

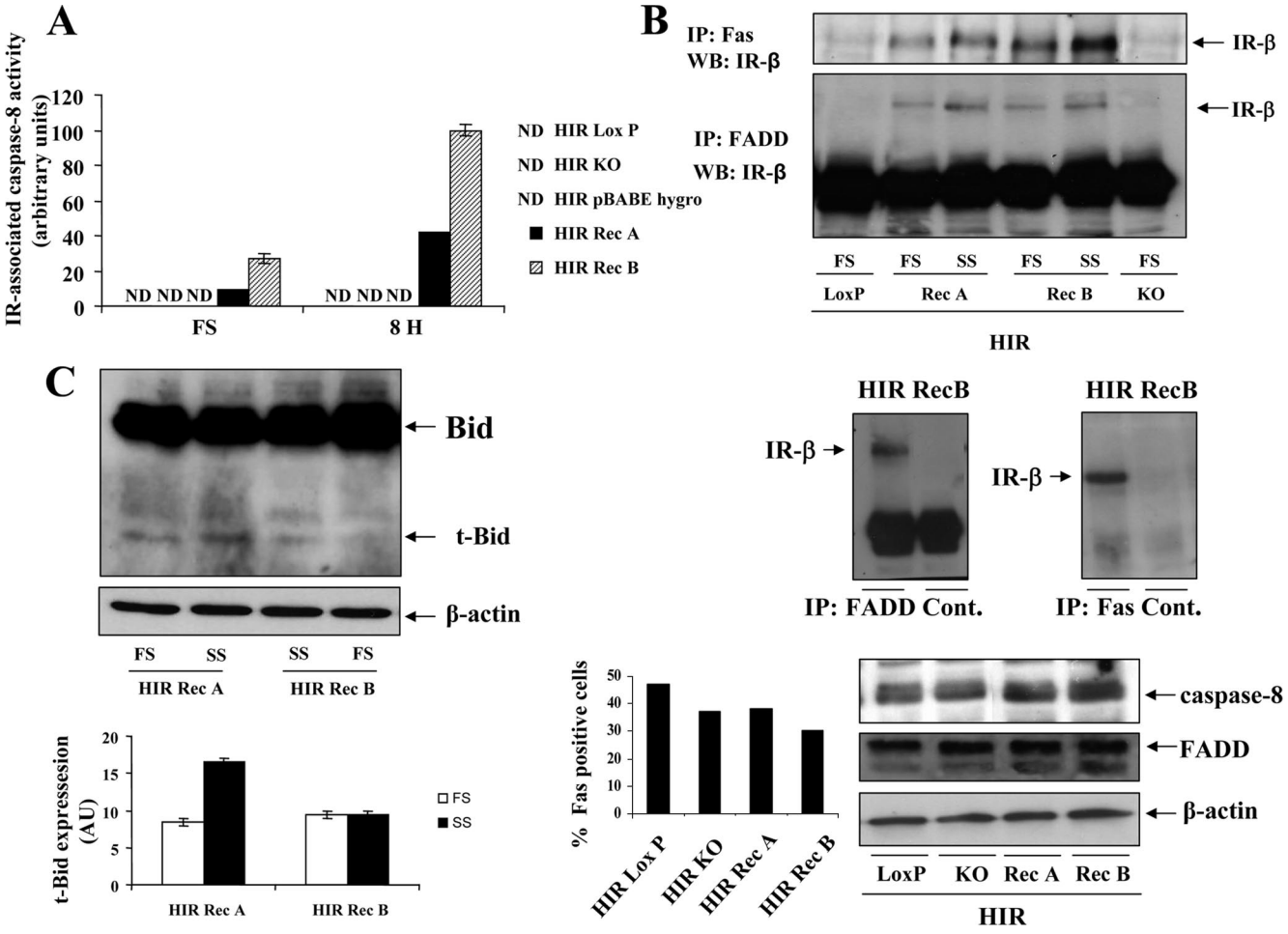

Figure 7. Immortalized hepatocytes expressing IRA and IRB isoforms associated caspase-8 activity, Fas, and FADD, but differentially induced Bid cleavage in response to serum withdrawal in immortalized hepatocytes. (A) Cells were serum deprived for 8 h. Some dishes were cultured in the presence of 10% FS. At the end of the culture time, adherent and nonadherent cells were collected and lysed as described in *Materials and Methods*. Equals amount of protein (1 mg) were immunoprecipitated with the anti-IR antibody. Caspase-8 activity was measured in the immune complexes as described in *Materials and Methods*. Results are expressed as arbitrary units, and they are means ± SE from four independent experiments with duplicate dishes. (B) Top, cells were serum-deprived for 8 h. At the end of the culture time, adherent and nonadherent cells were collected and lysed as described in *Materials and Methods*. Equals amount of protein (1 mg) were immunoprecipitated with anti-Fas or anti-FADD antibodies. The resulting immune complexes were analyzed by Western blot with the anti-IR antibody. A representative experiment is shown. Middle, control immunoprecipitations were performed with isotype serum (anti-hamster IgG as a control for anti-Fas immunoprecipitations and anti-rabbit IgG for anti-FADD immunoprecipitations). The immune complexes were analyzed by Western blot with the anti-IR antibody. Bottom, endogenous expression of FADD and caspase-8 was analyzed by Western blot. The cytometric quantification of Fas expression on the cell surface was analyzed as described in *Materials and Methods*. (C) Cells were cultured and lysed as described above. Total protein (50 μg) was submitted to SDS-PAGE and analyzed by immunoblotting with the corresponding antibodies against Bid and βactin. The expression of the truncated Bid fragment was indicated by an arrow. A representative experiment is shown. The autoradiograms corresponding to tBid expression were quantitated by scanning densitometry, and results are means ± SE from three independent experiments.

Figure 9A, levels of phosphorylated Akt and ERK were comparable to control HIR LoxP hepatocytes. Next, we investigated the susceptibility of HIR RecAB immortalized hepatocytes to undergo apoptosis upon growth factors withdrawal. For that goal, cells were deprived of serum for various times. Then, the percentage of apoptotic cells and the activities of caspases-8 and -3 were analyzed. Figure 9B shows that the coexpression of IRA and IRB resulted in a significant decrease in these parameters compared with IR-deficient hepatocytes. Of note, insulin was able to rescue HIR RecAB hepatocytes from serum-withdrawal-induced apoptosis. Finally, at the molecular level the coexpression of IRA and IRB resulted in a delay in Bim expression during the time course of serum withdrawal (Figure 9C).

DISCUSSION

Hepatoprotection remains one of the major challenges for clinical therapies aimed at limiting the liver damage induced by chronic hepatitis and cholestasis. It is now well established that most cells in higher animals may require continuous tropic stimulation to survive (Raff, 1992); otherwise, apoptosis occurs in response to withdrawal of serum/growth factors (Yao and Cooper, 1995, Stewart and Rotwein, 1996). Insulin promotes survival in a variety of cell types,

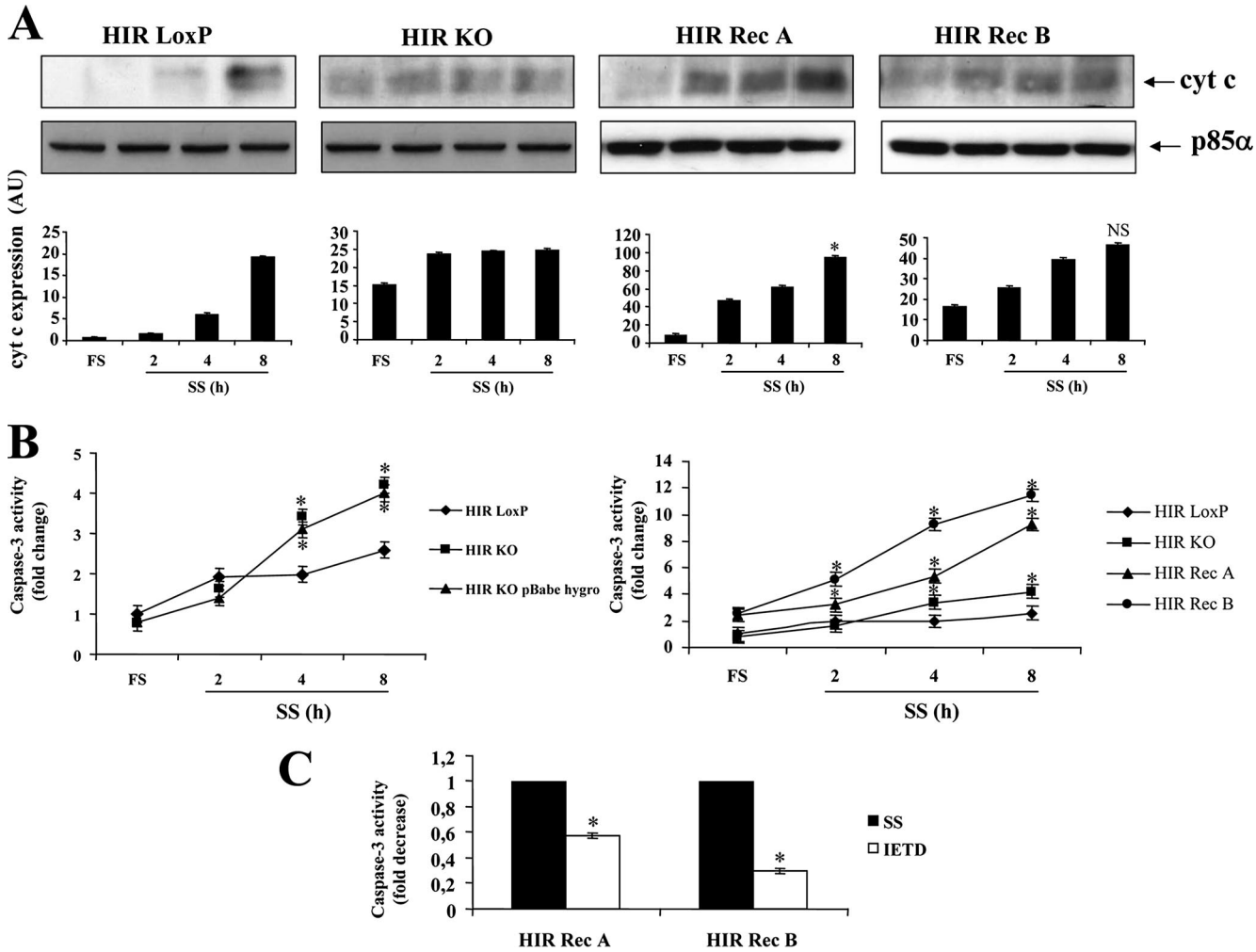

Figure 8. Differential effects on cytosolic cytochrome *c* release and caspase-3 activity in HIR KO immortalized hepatocytes reconstituted with isoforms A or B of IR. (A) HIR LoxP, HIR KO, HIR RecA, and HIR RecB immortalized hepatocytes were cultured under growing conditions (10% FS) or serum deprived for various times. Then, mitochondria were separated from cytosol, and cytochrome *c* content was analyzed in the cytosolic fraction by Western blot. Protein loading was visualized with the anti-p85α antibody. A representative experiment is shown. The autoradiograms corresponding to three independent experiments were quantitated by scanning densitometry, and results are means ± SE from three independent experiments. Statistical analysis was carried out by Student's *t* test by comparison between hepatocytes cultured in 10% FS and cells serum-deprived for 2–8 h (*$p < 0.05$). (B) Cells were serum-deprived for various times. At the end of the culture time, hepatocytes were collected and lysed. Caspase-3 activity was measured as described in *Materials and Methods*. The value corresponding to HIR LoxP hepatocytes, cultured in DMEM plus 10% FS, was set to 1. Results are expressed as -fold change of caspase-3 activity, and they are means ± SE from three independent experiments with duplicate dishes. Statistical analysis was carried out by Student's *t* test by comparison between IR-deficient (HIR KO and HIR KO pBabe hygro hepatocytes) and HIR LoxP cells (left) and between HIR RecA and HIR RecB hepatocytes and HIR KO cells (*$p < 0.05$). (C) HIR RecA and HIR RecB hepatocytes were cultured for 8 h in serum-free medium without or with 20 μM IETD. At the end of the culture time, caspase-3 activity was measured. The value corresponding to cells cultured in serum-free medium for 8 h was set to 1. Results are expressed as -fold decrease of caspase-3 activity, and they are means ± SE from three independent experiments with duplicate dishes. Statistical analysis was carried out by Student's *t* test by comparison between cells treated without and with IETD (*$p < 0.05$).

including SV40-immortalized neonatal hepatocytes (Valverde *et al*., 2004). The biological effects of insulin in its target tissues are mediated by a complex network of intracellular signaling pathways initiated by the activation of the IR at the cell surface. In this regard, SV40-immortalized neonatal hepatocytes lacking IR (HIR KO) are useful tools to study the role of IR signaling in the protection against apoptosis. Interestingly, these cells maintain phenotypical characteristics of control (HIR LoxP) hepatocytes (Nevado *et al*., 2006). In the present study, we demonstrate that IR deficiency in immortalized hepatocytes is associated with accelerated apoptosis in response to withdrawal of growth factors. As immortalized neonatal hepatocytes bearing or not IR express similar levels of IGF-IR, the results presented here indicate that the lack of IR cannot be compensated by the IGF-IR and its signaling, thereby excluding functional redundancy of these receptors in hepatocytes during fetal development.

Insulin-mediated phosphorylation of Akt and ERK, two major survival pathways in mammalian cells (Rosseland *et al*., 2005; Luedde and Trautwein, 2006), was virtually absent in immortalized IR-deficient hepatocytes, but it was rescued by the expression of either IRA or IRB isoform. These results strongly indicate that either isoform when expressed in

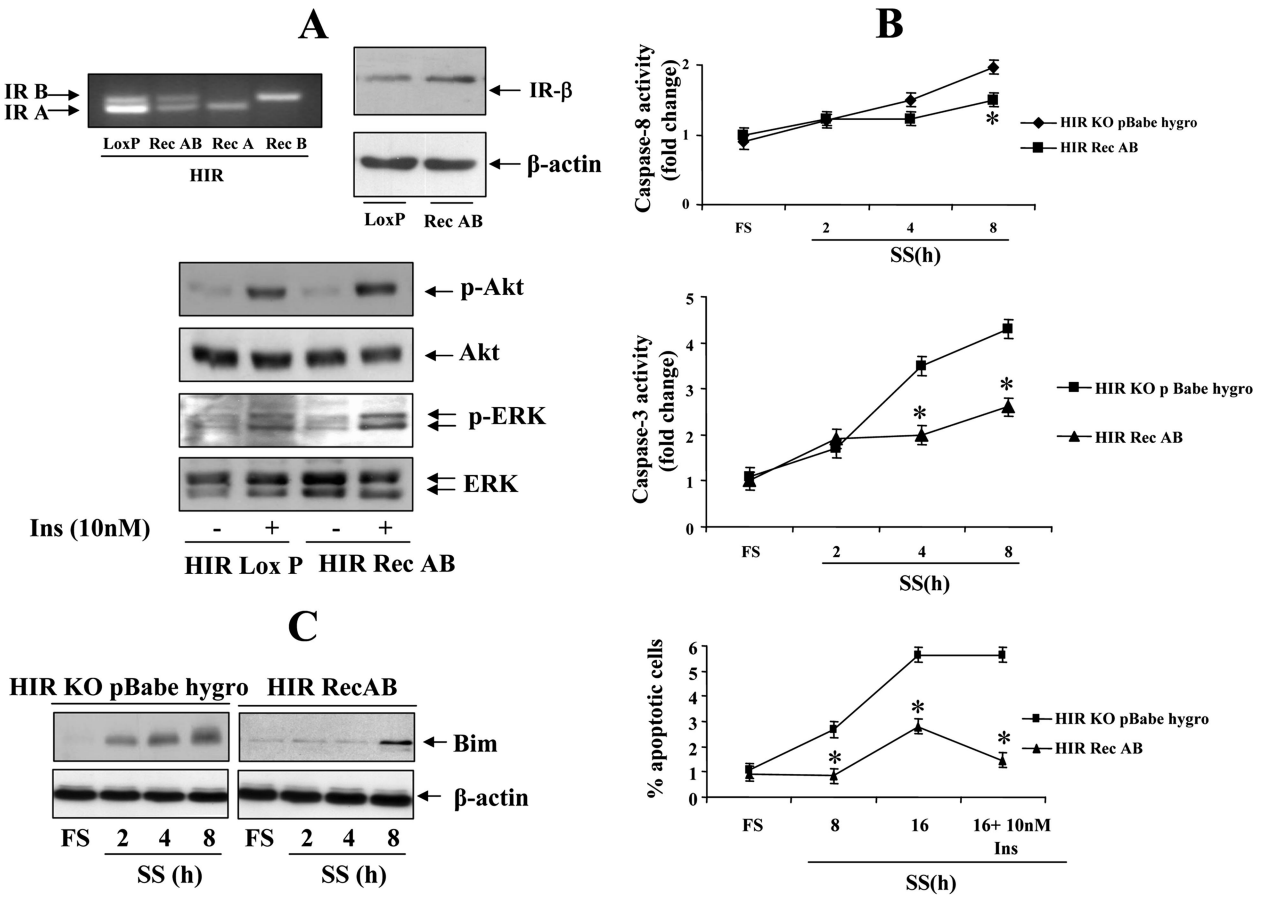

Figure 9. Coexpression of IRA and IRB in immortalized IR-deficient hepatocytes reverted the susceptibility to undergo apoptosis upon growth factors deprivation. (A) Representative RT-PCR and western blot of IR in HIR RecAB and HIR LoxP hepatocytes. Cells were cultured in DMEM plus 10% FS to 90% confluence, serum starved for 4 h, and stimulated with 10 nM insulin for 10 min. Control cells were cultured in the absence of the hormone. At the end of the culture time, cells were lysed and total protein (50 μg) was analyzed by Western blot with the anti-phospho-Akt (Ser473) and phospho ERK (Thr 202/Tyr 204) antibodies. The autoradiograms shown are representative of three experiments. (B) Top, HIR RecAB and HIR KO pBabe hygro hepatocytes were serum deprived for various times. Then, caspase-8 and -3 activities were analyzed. The value corresponding to HIR KO pBabe hygro hepatocytes, cultured in DMEM plus 10% FS, was set to 1. Results are expressed as -fold change of caspase-8 and -3 activities, and they are means ± SE from three independent experiments with duplicate dishes. Statistical analysis was carried out by Student's *t* test by comparison between HIR KO pBabe hygro and HIR RecAB hepatocytes (*$p < 0.05$). Bottom, cells were serum starved for various times. Some dishes were cultured with insulin for 16 h. Results are expressed as percentage of apoptotic cells, and they are means ± SE from three independent experiments with duplicate dishes. Statistical analysis was carried out by Student's *t* test by comparison between HIR KO pBabe hygro and HIR RecAB hepatocytes (*$p < 0.05$). (C) Cells were serum-deprived for the indicated times. Total protein (50 μg) was used for Western blot analysis with the antibodies against Bim and β-actin for protein loading. A representative experiment is shown.

hepatocytes is completely functional in terms of insulin signaling. Indeed, when cultured in serum-free medium, but in the presence of insulin, these cell lines were fully protected from apoptosis. These results confirm that activation of Akt and ERK signaling pathways by either isoform of IR enables survival in immortalized hepatocytes. In sharp contrast, when hepatocytes expressing only IRA or IRB were subjected to a time course of serum withdrawal, the rate of apoptosis was increased as compared with IR-deficient cells. In humans and mice, IR isoform expression is tightly regulated by development. For example, in human fetal tissues a clear shift from IRA to IRB was reported in muscle, liver, and kidney (Frasca *et al*., 1999), whereas adult liver expressed only IRB (Giddings and Carnaghi, 1992). Thus, as discussed above, cells bearing a severe imbalance in the expression of IRA and IRB isoforms during a particular stage of development, such as the neonatal period, might be more susceptible to programmed cell death to prevent structural or functional alterations in developing tissues.

Serum withdrawal is a stimulus that induces apoptosis by elevating cellular ROS levels (Lee *et al*., 2005). In the current study, we have evaluated whether the lack of IR and serum withdrawal can synergize to promote oxidant injury and cellular toxicity in immortalized hepatocytes. Indeed, under our experimental conditions, IR-deficient cells displayed a time-dependent increase in ROS levels. Importantly, this effect was totally avoided by expression of either isoform A or B of the IR or both. Therefore, the generation of ROS as a possible mechanism by which individual expression of IRA or IRB triggers apoptosis can be ruled out in immortalized neonatal hepatocytes.

In mammalian cells, apoptosis proceeds along the extrinsic (death receptor) or the intrinsic (mitochondrial) pathways that broadly interact with each other (Danial and Korsmeyer, 2004). The extrinsic pathway is activated by the engagement of death receptors on the cell surface. The intrinsic pathway is triggered by various extracellular and intracellular stress signals, such as growth factor with-

drawal, hypoxia, DNA damage, and oncogene induction resulting in the permeabilization of the outer mitochondrial membrane, the release of cytochrome *c* and other proapoptotic molecules, the formation of the apoptosome, and caspase activation. Among these processes, only the permeabilization step is regulated, given that antiapoptotic members of the Bcl family can block progression of apoptotic death (Okada and Mak, 2004). Immortalized hepatocytes grown in 10% FS express high levels of the antiapoptotic member Bcl-x_L, which prevent cytochrome *c* release from mitochondria to the cytosol. The lack of IR down-regulated endogenous Bcl-x_L expression; interestingly, this effect was not rescued by the expression of IRA or IRB isoforms. By contrast, the expression of the proapoptotic members Bim and Bid was similar between all the cell lines. These results clearly indicate that the lack of IR in immortalized hepatocytes creates an imbalance between endogenous pro- and antiapoptotic genes, which may accelerate the sequential cellular events leading to DNA fragmentation and apoptosis. On serum withdrawal, Bim is a proapoptotic protein that is highly induced in a number of cell types, including immortalized hepatocytes (Valverde *et al*., 2004). Our results demonstrate that serum withdrawal stimulates a time-dependent increase in Bim expression in control cells. When IR was absent, Bim was up-regulated more rapidly in response to serum deprivation. However, our results clearly indicate that the up-regulation of Bim is not the molecular mechanism by which apoptosis is enhanced in HIR RecA or HIR RecB hepatocytes.

In contrast to the family of Bcl-related proteins, less is known about the role of Foxo proteins in the mechanism of apoptosis. In the absence of Akt signaling, these proteins localize predominantly to the nucleus where they bind to promoters of target genes that induce cell death including FasL (Suhara *et al*., 2002) and Bim (Dijkers *et al*., 2000; Stahl *et al*., 2002). Indeed, overexpression of Foxo1 or Foxo3a induces apoptosis in various cell types, including immortalized neonatal hepatocytes (Brunet *et al*., 1999; Tang *et al*., 1999; Valverde *et al*., 2004). In cells cultured under serum-free conditions, nuclear localization of Foxo1 is accelerated by the lack of IR. This effect, together with the acceleration of Bim expression, might contribute to the acceleration of cytochrome *c* release, the increase in caspase-3 activity, and the increased susceptibility to apoptosis induced by serum withdrawal in IR-deficient immortalized hepatocytes. These results together with our previous reports (Valverde *et al*., 2004, Gonzalez-Rodriguez *et al*., 2007) show a positive correlation between Akt/Foxo1 phosphorylation and survival in hepatocytes. However, because no significant alterations in the accumulation of Foxo1 in the nucleus were found in HIR RecA or HIR RecB hepatocytes, the involvement of this molecular mechanism in the apoptosis induced by the individual expression of IR isoforms should be minimal. Moreover, because mammalian target of rapamycin is a downstream target of Akt that controls cell growth, the contribution of this pathway to the regulation of apoptosis in hepatocytes should not be excluded.

Apoptosis induced by serum withdrawal is partly due to increased FasL signaling that is regulated by nuclear Foxo1 (Suhara *et al*., 2002). Because the accumulation of nuclear Foxo1 was accelerated in serum-deprived immortalized hepatocytes lacking IR, caspase-8 activity was also slightly higher compared with the control HIR LoxP cell line. Notably, caspase-8 activity was much elevated in hepatocytes expressing either IRA or IRB isoform at all the time points of serum withdrawal. This result was unexpected, because the time course of the accumulation of nuclear Foxo1 was similar as in HIR KO cells, as discussed above. More importantly, the fact that the high percentage of apoptotic cells induced by 8 h of serum withdrawal was suppressed by incubation with IETD indicates that the activation of caspase-8, by a Foxo1-independent mechanism, induced directly the apoptosis in HIR RecA or HIR RecB hepatocytes. Moreover, we found a significant increase in caspase-8 activity associated with anti-IR immune complexes in immortalized hepatocytes expressing IRA or IRB, but not in control or IR-deficient cells, after 8 h of serum withdrawal. Because caspase-8 is activated exclusively by the death receptor pathway, we investigated the possibility that IR isoforms form complexes that include membrane death receptors.

Studies in patients and animal models strongly suggest that the death receptor cascade mediated by Fas/FasL is involved in the induction of apoptosis and the consequent liver damage (Luedde *et al*., 2002). On ligand binding, Fas recruits the death-inducing signaling complex (DISC) (Barnhart *et al*., 2003). The DISC complex consists on the Fas receptor, procaspase-8, procaspase-10, and FADD. Our results clearly demonstrate the presence of IRA/Fas/FADD or IRB/Fas/FADD protein complexes under basal conditions. More importantly, those complexes were more abundant upon 8 h of serum deprivation in parallel to the activation of IR-associated caspase-8. This effect was more marked in immortalized hepatocytes expressing IRB. Importantly, the increase in caspase-8 activity was not the result of increased caspase-8 levels. Indeed, the formation of these complexes parallels an intense activation of caspase-3 that is inhibited by IETD, reinforcing the idea that activation of IRA/Fas/FADD or IRB/Fas/FADD complexes can trigger a death receptor signaling. The complex formed between tyrosine kinase membrane receptors and death molecules has been recently reported by Ling et al. (2006). These authors have found that RIP, a critical effector of TNF receptor signaling, is recruited into the IGF-IR signaling complex in a ligand-dependent manner.

Autoproteolytic cleavage of caspase-8 is an early detectable event in Fas-induced apoptosis, leading to caspase-3 activation either in a mitochondria-independent manner or via a mitochondria-dependent pathway that proceeds via Bid and caspase-9 (Scaffidi *et al*., 1998, 1999). Our results reveal a significant increase of Bid cleavage in parallel with an increase in cytochrome *c* release at 8 h of serum withdrawal in HIR RecA cells, compared with HIR KO hepatocytes. These data suggest that the mitochondria-dependent pathway might participate in the apoptosis mediated by IRA/Fas/FADD complexes. By contrast, the fact that in HIR RecB cells the time course of cytochrome *c* release is similar to that of HIR KO hepatocytes suggest that the direct activation by the initiator caspase-8 might be the mechanism by which the executioner caspase-3, and, ultimately, cell death is activated by IRB/Fas/FADD complexes. Efficient execution of apoptosis requires an adequate supply of ATP (Dey and Moraes, 2000). This is particularly important in kidney and colon carcinomas because the selective repression of β-F1-ATPase expression hampered the apoptotic potential of the cancer cells, resulting in chemo- and radiotherapy resistance (Cuezva *et al*., 2002). In a recent study, we have demonstrated that hepatocytes expressing only IRA have increased rate of glucose entry compared with those expressing IRB. This difference in glucose disposal could lead to more ATP availability in HIR RecA cells, thereby enabling formation of the apoptosome and mitochondrial-dependent caspase-3 activation. Therefore, in immortalized hepatocytes expressing IRB, the lower glucose/ATP availability might limit apoptosome formation, permitting the direct activation of caspase-3 by caspase-8.

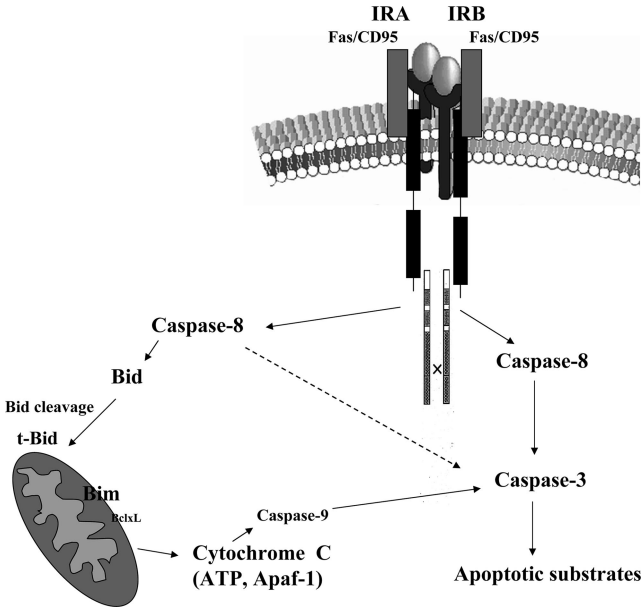

Figure 10. Molecular model of the differential apoptotic mechanism in serum-deprived HIR RecA or HIR RecB immortalized hepatocytes. In serum-deprived HIR RecB hepatocytes, the complex IRB/Fas/FADD triggers caspase-8 activation at the disk, which might bypass mitochondria, directly activating caspase-3 and subsequently apoptosis. In HIR RecA neonatal hepatocytes, the complex IRA/Fas/FADD leads to the activation of caspase-8, Bid cleavage, and the apoptogenic function of mitochondria resulting in cytochrome *c* release and caspase-3 activation. Of note, in this model the expression levels of IR in HIR RecA and HIR RecB immortalized hepatocytes may also play a role.

Although the results presented in this study are the first evidence of the unique role of IR isoforms in the regulation of programmed cell death, changes in IRA/IRB ratio have been reported in several diseases such as type 2 diabetes and cancer. Particularly, there are studies showing that there is a preferential expression of IRA in many types of cancer including those of the lung, colon, breast, ovaries, thyroid, and smooth and striated muscle (reviewed in Denley *et al*., 2003). The IRB is also down-regulated in hepatoblastomas (von Horn *et al*., 2001). In immortalized neonatal hepatocytes, coexpression of IRA and IRB isoforms rescued from the susceptibility to undergo apoptosis provoked by the individual expression of either IR isoform. These results together with the activation of the apoptotic pathways summarized in Figure 10 reinforce the idea that the expression of IRA and IRB isoforms must be tightly regulated through development for the protection against cell death in hepatocytes. Whether or not an imbalance in IRA/IRB ratio could affect hepatoprotection in humans will require further investigations.

ACKNOWLEDGMENTS

We acknowledge Luis Goya (Instituto de Frio, Consejo Superior de Investigaciones Cientificas, Spain) for the determination of ROS and Javier Naval (University of Zaragoza, Spain) for the suggestions and the supply of Jo2. This work was supported by grants SAF 2004-5545 (to M.B.), BFU 2005-1615 (to A.M.V.), and CIBERDEM, Instituto Carlos III, M.S.C. (Spain).

REFERENCES

Alia, M., Ramos, S., Mateos, R., Bravo, L., and Goya, L. (2006). Quercetin protects human hepatoma cell line (HepG2) against oxidative stress induced by tertbutyl hydroperoxide. Toxicol. Appl. Pharmacol. *212*, 110–118.

Barnhart, B. C., Alappat, E. C., and Peter, M. E. (2003). CD95 type I/type II model. Semin. Immunol. *15*, 185–193.

Brunet, A., Bonni, A., Zigmond, M. J., Lin, M. Z., Juo, P., Hu, L. S., Anderson, M. J., Arden, K. C., Blenis, J., and Greenberg, M. E. (1999). Akt promotes cell survival by phosphorylating and inhibiting a Forkhead transcription factor. Cell *96*, 857–868.

Cuezva, J. M., Krajewska, M., de Heredia, M. L., Krajewski, S., Santamaría, G., Kim, H., Zapata, J. M., Marusawa, H., Chamorro, M., and Reed, J. C. (2002). The bioenergetic signature of cancer: a marker of tumor progression. Cancer Res. *62*, 6674–6681.

Danial, N. N., and Korsmeyer, S. J. (2004). Cell death: critical control points. Cell *103*, 205–219.

Denley, A., Wallace, J. C., Cosgrove, L. J., and Forbes, B. E. (2003). The insulin receptor isoform exon 11- (IR-A) in cancer and other diseases: a review. Horm. Metab. Res. *35*, 778–785.

Dey, R., and Moraes, C. T. (2000). Lack of oxidative phosphorylation and low mitochondrial membrane potential decrease susceptibility to apoptosis and do not modulate the protective effect of Bcl-x(L) in osteosarcoma cells. J. Biol. Chem. *275*, 7087–7094.

Dijkers, P. F., Medema, R. H., Lammers, J. W., Koenderman, L., and Coffer, P. J. (2000). Expression of the pro-apoptotic Bcl-2 family member Bim is regulated by the forkhead transcription factor FKHR-L1. Curr. Biol. *10*, 1201–1204.

Entingh, A. J., Taniguchi, C. M., and Kahn, C. R. (2003). Bi-directional regulation of brown fat adipogenesis by the insulin receptor. J. Biol. Chem. *278*, 33377–33383.

Fabregat, I., Lorenzo, M., and Benito, M. (1989). Precocious induction of malic enzyme by nutritional and hormonal factors in rat fetal hepatocyte primary cultures. Biochem. Biophys. Res. Commun. *161*, 1028–1034.

Frasca, F., Pandini, G., Scalia, P., Sciacca, L., Mineo, R., Costantino, A., Goldfine, I. D., Belfiore, A., and Vigneri, R. (1999). Insulin receptor isoform A, a newly recognized, high-affinity insulin-like growth factor II receptor in fetal and cancer cells. Mol. Cell. Biol. *19*, 3278–3288.

Giddings, S. J., and Carnaghi, L. R. (1992). Insulin receptor gene expression during development: developmental regulation of insulin receptor mRNA abundance in embryonic rat liver and yolk sac, developmental regulation of insulin receptor gene splicing, and comparison to abundance of insulin-like growth factor 1 receptor mRNA. Mol. Endocrinol. *6*, 1665–1672.

Goldstein, B. J., and Dudley, A. L. (1990). The rat insulin receptor: primary structure and conservation of tissue-specific alternative messenger RNA splicing. Mol. Endocrinol. *4*, 235–244.

Gonzalez-Rodriguez, A., Escribano, O., Benito, M., Rondinone, C., and Valverde, A. M. (2007). Levels of protein tyrosine phosphatase 1B determine the susceptibility to apoptosis in PTP1B-defincient hepatocytes. J. Cell. Physiol. *212*, 76–88.

Guillén, C., Navarro, P., Robledo, M., Valverde, A. M. and Benito, M. (2006). Differential mitogenic signaling in insulin receptor-deficient fetal pancreatic beta-cells. Endocrinology *147*, 1959–1968.

Juo, P., Kuo, C. J., Yuan, J., and Blenis, J. (1998). Essential requirement for caspase-8/FLICE in the initiation of the Fas-induced apoptotic cascade. Curr. Biol. *8*, 1001–1008.

Kennedy, S. G., Wagner, A. J., Conzen, S. D., Jordan, J., Bellacosa, A., Tsichlis, P. N., and Hay, N. (1997). The PI3 kinase/Akt signalling pathway delivers an antiapoptotic signal. Genes Dev. *11*, 701–713.

Kosaki, A., and Webster, N.J.G. (1993). Effect of dexamethasone on the alternative splicing of the insulin receptor mRNA and insulin action in HepG2 hepatoma cells. J. Biol. Chem. *268*, 21990–21996.

Lee, S. B., Hong, S. H., Kim, H., and Um, H. D. (2005). Co-induction of cell death and survival pathways by phosphoinositide 3-kinase. Life Sci. *78*, 91–98.

Ling, Y., Yang, Q., Wang, X., and Liu, Z. (2006). The essential role of the death domain kinase receptor-interacting protein in insulin growth factor-I-induced c-Jun N-terminal kinase activation. J. Biol. Chem. *281*, 23525–23532.

Luedde, T. and Trautwein, C. (2006). Intracellular survival pathways in the liver. Liver Int. *26*, 1163–1174.

Luedde, T., Liedtke, C., Manns, M. P., and Trautwein, C. (2002). Losing balance: cytokine signalling and cell death in the context of hepatocyte injury and hepatic failure. Eur. Cytokine Netw. *13*, 377–383.

Lyons, A. B., Samuel, K., Sanderson, A., and Maddy, A. H. (1992). Simultaneous analysis of immunophenotype and apoptosis of murine thymocytes by single laser flow cytometry. Cytometry *13*, 809–821.

Malhi, H., Gores, G. J., and Lemasters, J. J. (2006). Apoptosis and necrosis in the liver: a tale of two deaths?. Hepatology *43* (2 Suppl 1), S31–S44.

Michael, M. D., Kulkarni, R. N., Postic, C., Previs, S. F., Shulman, G. I., Magnuson, M. A., and Kahn, C. R. (2000). Loss of insulin signaling in hepatocytes leads to severe insulin resistance and progressive hepatic dysfunction. Mol. Cell *6*, 87–97.

Moller, D. E., Yokota, A., Caro, J. F., and Flier, J. S. (1989). Tissue-specific expression of two alternatively spliced insulin receptor mRNAs in man. Mol. Endocrinol. *3*, 1263–1269.

Nakae, J., Barr, V., and Accili, D. (2000). Differential regulation of gene expression by insulin and IGF-1 receptors correlates with phosphorylation of a single amino acid residue in the forkhead transcription factor FKHR. EMBO J. *19*, 989–996.

Nevado, C., Valverde, A. M., and Benito, M. (2006). Role of insulin receptor in the regulation of glucose uptake in neonatal hepatocytes. Endocrinology *147*, 3709–3718.

Okada, H., and Mak, T. W. (2004). Pathways of apoptotic and non-apoptotic death in tumour cells. Nat. Rev. Cancer *4*, 592–603.

Ockner, R. K. (2001). Apoptosis and liver diseases: recent concepts of mechanism and significance. J. Gastroenterol. Hepatol. *16*, 248–260.

Patel, T., Roberts, L. R., Jones, B. A., and Gores, G. J. (1998). Dysregulation of apoptosis as a mechanism of liver disease: an overview. Semin. Liver Dis. *18*, 105–114.

Raff, M. (1992). Social controls on cell survival and cell death. Nature *356*, 397–400.

Rosseland, C. M., Wierod, L., Oksvold, M. P., Werner, H., Ostvold, A. C., Thoresen, G. H., Paulsen, R. E., Huitfeldt, H. S., and Skarpen, E. (2005). Cytoplasmic retention of peroxide-activated ERK provides survival in primary cultures of rat hepatocytes. Hepatology *42*, 200–207.

Scaffidi, C., Fulda, S., Srinivasan, A., Friesen, C., Li, F., Tomaselli, K. J., Debatin, K. M., Krammer, P. H., and Peter, M. E. (1998). Two CD95 (APO-1/Fas) signaling pathways. EMBO J. *17*, 1675–1687.

Scaffidi, C., Schimitz, I., Zha, J., Korsmeyer, S. J., Krammer, P. H., and Peter, M. E. (1999). Differential modulation of apoptosis sensitivity in CD95 type I and type II cells. J. Biol. Chem. *274*, 22532–22538.

Schulte-Hermann, R., Bursch, W., Low-Baseli, A., Wagner, A., and Grasl-Kraupp, B. (1997). Apoptosis in the liver and its role in carcinogenesis. Cell. Biol. Toxicol. *13*, 339–348.

Seino, S., and Bell, G. I. (1989). Alternative splicing of human insulin receptor messenger RNA. Biochem. Biophys. Res. Commun. *159*, 312–316.

Stahl, M., Dijkers, P. F., Kops, G. J., Lens, S. M., Coffer, P. J., Burgering, B. M., and Medema, R. H. (2002). The forkhead transcription factor FoxO regulates transcription of p27Kip1 and Bim in response to IL-2. J. Immunol. *168*, 5024–5031.

Stewart, C. E., and Rotwein, P. (1996). Insulin-like growth factor-II is an autocrine survival factor for differentiating myoblasts. J. Biol. Chem. *271*, 11330–11338.

Suhara, T., Kim, H. S., Kirshenbaum, L. A., and Walsh, K. (2002). Suppression of Akt signaling induces Fas ligand expression: involvement of caspase and Jun kinase activation in Akt-mediated Fas ligand regulation. Mol. Cell. Biol. *22*, 680–691.

Tang, E. D., Nunez, G., Barr, F. G., and Guan, K. L. (1999). Negative regulation of the forkhead transcription factor FKHR by Akt. J. Biol. Chem. *27*, 16741–16746.

Valverde, A. M., Fabregat, I., Burks, D. J., White, M. F., and Benito, M. (2004). IRS-2 mediates the anti-apoptotic effect of insulin in neonatal hepatocytes. Hepatology *40*, 1285–1294.

Valverde, A. M., Burks, D., Fabregat, I., Fisher, C., Carretero, J., White, M. F., and Benito, M. (2003). Molecular mechanisms of insulin resistance in IRS-2-deficient hepatocytes. Diabetes *52*, 2239–2248.

von Horn, H., Tally, M., Hall, K., Eriksson, T., Ekstrom, T. J., and Gray, S. G. (2001). Expression levels of insulin-like growth factor binding proteins and insulin receptor in hepatoblastomas. Cancer Lett. *162*, 253–260.

Wang, H., and Joseph, J. A. (1999). Quantifying cellular oxidative stress by dichlorofluorescein assay using microplate reader. Free Radic. Biol. Med. *27*, 612–616.

Yao, R., and Cooper, G. M. (1995). Requirement for phosphatidylinositol-3 kinase in the prevention of apoptosis by nerve growth factor. Science *267*, 2003–2006.